

# HELIUM EMISSION IN THE MIDDLE CHROMOSPHERE

M. A. LIVSHITS

*Institute of Terrestrial Magnetism, Ionosphere and Radio Wave Propagation (IZMIRAN), near Moscow*

and

L. A. AKIMOV, I. L. BELKINA, and N. P. DYATEL

*Astronomical Observatory of Kharkov University, Kharkov*

(Received 11 November, 1975)

**Abstract.** Slitless spectrograms obtained during the eclipse of 10 June 1972 have been analyzed to determine the height distribution of the  $D_3$  He line intensity.

For undisturbed regions the maximum of  $D_3$  line intensity is confirmed to exist at about 1700 km above the limb. Besides the above mentioned maximum, in plages a considerable intensity may be observed at low heights ( $h < 1000$  km).

An analysis of these observations for  $h > 1000$  km has been carried out within the low temperature mechanism of triplet helium emission taking into account the helium ionization by XUV radiation. The density dependence of the  $2^3S$  level population at different XUV flux values has been calculated. Our observations give  $N_e \approx 2 \times 10^{10} \text{ cm}^{-3}$  in the chromosphere at  $h = 2000$  km. The probable coincidence of the H and He emission small filaments in the middle chromosphere is discussed.

## 1. Observational data

The helium  $D_3$  emission at different heights over the limb was observed by expeditions from the Astronomical observatory of Kharkov University during the solar eclipses of 22 September 1968 and 10 July 1972. Preliminary results of the observations of the 1968 eclipses were given by Belkina and Dyatel (1972), here referred to as Paper 1. In 1972 the slitless spectrograph contained a diffraction grating ( $600 \text{ mm}^{-1}$ ,  $100 \times 100 \text{ mm}^2$ ) and the objective of the camera had  $D = 100$  mm and  $F = 800$  mm. In 1972 the spectrograph had a dispersion of  $18 \text{ \AA/mm}$  and made 10–26 exposures per second (12–35 km intervals in the chromosphere). The time of the exposure was registered exactly. The instrumentation and data reduction procedure were discussed in detail in Paper 1. The spectra near the second and the third contacts of the eclipse of 10 July 1972 were obtained under good atmospheric conditions. The structure of He and Na lines was clearly revealed (Figure 1).

In this paper the photometric analysis of 650 spectra near the second contact of the 1972 eclipse is given. The microphotometer slit covered about 10 000 km along the solar limb in the direction perpendicular to the dispersion. The zero-point of the height scale was determined from the measurements of  $D_1$ ,



Fig. 1. The flash spectrum near the second contact of 1972 eclipse. The minimum height of radiating points is about 700 km. The large prominence is situated southwards.

$D_2$  Na lines. Following Gulyaev (1971), we assumed the maximum intensity of  $D_1$ ,  $D_2$  lines to occur at  $h = -100$  km. According to Gulyaev, the accuracy of zero-point determination is of the order of several tens of kilometers. For some point along the limb the zero-points were verified by measurements of the limb darkening, as for Paper 1. Photometric scans were essentially made in such a way that the center of the photometer slit coincided with the middle of Baily's beads. Thus, the errors caused by inaccurate matching of points in different spectra were reduced to a minimum. The region characterized by nearly homogeneous luminosity and situated between the point of the second contact and the heliographic latitude  $40^\circ\text{N}$  was studied. Locations of points are given in Table I.

From the analysis of  $H\alpha$ , H and K Ca II filtergrams obtained during 10–13 July 1972 it follows that the limb in the range  $\rho = 55\text{--}65^\circ$  was undisturbed. Points 8–12 correspond to undisturbed regions.

TABLE I  
Position angles ( $\rho$ ) and heliographic latitudes  
( $\varphi$ ) for selected points

Point numbers	Position angles ( $\rho$ )	Heliographic latitudes ( $\varphi$ )
1	86.3	+5.4
2	84.1	+7.6
3	80.7	+11.0
4	78.2	+13.5
5	73.9	+17.8
6	71.6	+20.1
7	70.0	+21.7
8	63.2	+28.5
9	60.2	+31.5
10	58.4	+33.5
11	56.9	+34.8
12	54.7	+37.0

There was McMath 11936 on the E-limb on the day of the eclipse. According to *Solar Geophysical Data* (1972), this plage covered the range  $72^\circ < \rho < 83^\circ$  and had a small spot near  $\rho \approx 82^\circ$ . It was probably the return of McMath 11928 (it also follows from the picture of the plage). At  $\rho > 70^\circ$  a faint coronal condensation in red and green lines was observed, having its maximum at  $\rho \approx 85^\circ$  (Poulain, 1974). By using the slit spectrograms, Shilova (1973) studied a rather dense chromospheric feature which was located near the point of the second contact at  $\rho = 80^\circ$ . We believe that points with  $\rho > 70^\circ$  may be attributed to the faint active regions.

Figure 2 gives the observed values of  $E$  (surface brightness integrated radially above the limb of the Moon) in  $\text{ergs cm}^{-1} \text{s}^{-1} \text{sterad}^{-1}$  for twelve studied points. The relationship of  $E$  with the activity on the limb is clearly shown. At heights from 2000 to 4000 km the value  $E(h)$  decreased steadily at almost the same rate for all points. But at low heights in undisturbed regions ( $\rho < 65^\circ$ ), with decreasing  $h$ , the  $E(h)$  curves flatten out into a 'plateau' with a maximum less than  $4 \times 10^{13}$   $\text{ergs cm}^{-1} \text{s}^{-1} \text{sterad}^{-1}$ . In the case of the plage, with decreasing  $h$ , the value  $E(h)$  goes on increasing up to  $12 \times 10^{13}$   $\text{ergs cm}^{-1} \text{s}^{-1} \text{sterad}^{-1}$ .

It should be noted that the absolute values of  $E(h)$  for the undisturbed regions under discussion slightly exceed the value  $E(h)$  determined by Gulyaev (1971) for the undisturbed E-limb of the 1968 eclipse, but are slightly below the value of  $E(h)$  of the least disturbed regions of W-limb (Paper 1). Comparison with early independent absolute determinations of  $E(h)$  was made in Paper 1.

The function  $I(h)$  for individual points is determined without certainty due to photometric errors and errors of numerical differentiation. However, as follows from our data for both eclipses (1968 and 1972), all  $I(h)$  curves are divided into two groups according to their shapes, corresponding to the active and the

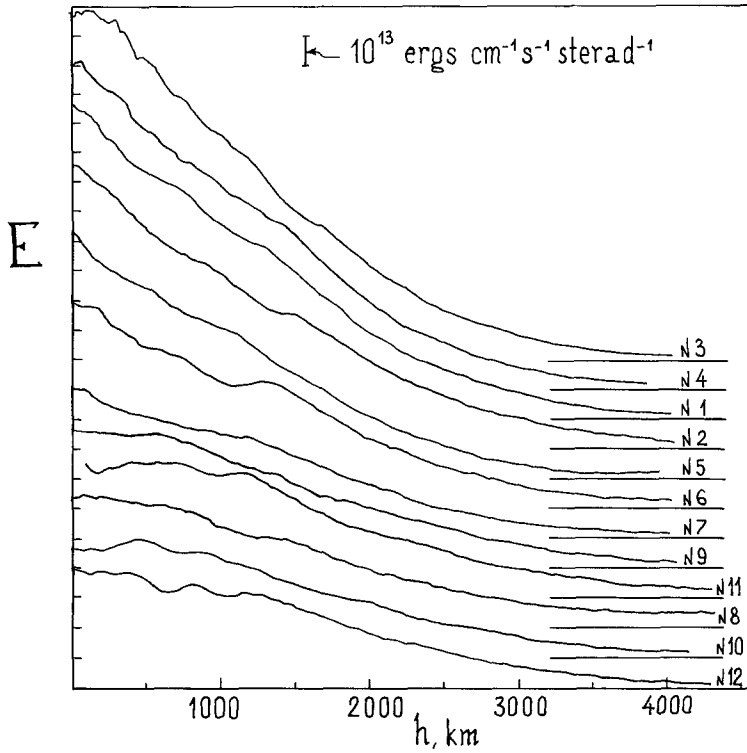


Fig. 2.  $D_3$  observation of the 12 points under consideration. Absciss axes for each point are shifted by  $10^{13} \text{ ergs cm}^{-1} \text{ s}^{-1} \text{ sterad}^{-1}$  relative to one another. Parts of the axes are shown in the right side of the figure. The number above the axis indicates the number of the point in Table I.

undisturbed chromosphere. (The function  $I(h)$  in the chromosphere immediately above the small spots has a very complicated shape). Such a division of  $I(h)$  curves makes it possible to average the derivatives for 8–12 points (undisturbed chromosphere) and for 1–7 points (faint plage). The results are given in Figure 3. In undisturbed regions with smaller values of  $I(h)$  this function reaches its

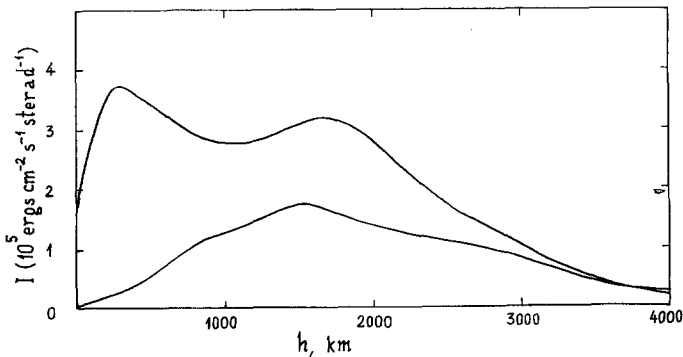


Fig. 3. Surface brightness for undisturbed region (the lower curve) and faint plage (the upper curve).

maximum at  $h \approx 1700$  km. This fact is important for clearing up the helium emission mechanism. The existence of this maximum was suggested by the data in previous works by White (1963), Gulyaev (1971) and Belkina *et al.* (1972). In this paper the maximum was derived from the data obtained in the height range up to 4000 km. Besides the maximum at 1700–1900 km, there is some excess of radiation at  $h < 1000$  km in faint plages. It seems that the contribution of radiation from such low heights increases when passing from an undisturbed region to a more active one. More accurate analysis consisting in the application of different averaging techniques to differentiation and estimation of photometric errors revealed the reality of both maxima. For a definite solution of that question it would be desirable to compare the functions  $I(h)$  in some points of the limb determined by independent experiments.

### 2. Analysis of Data

We shall discuss only the data for  $h > 1000$  km. In a spherically symmetric atmosphere the  $D_3$  line emission coefficient may be obtained from the Abelian type equation (see, for example, Sobolev, 1967)

$$\epsilon(h) = -\frac{1}{\pi(2R_\odot)^{1/2}} \frac{d}{dh} \int_h^\infty \frac{I(z)}{(z-h)^{1/2}} dz, \tag{1}$$

where  $z$  is the radial height of a point on the line of sight above the base of the chromosphere,  $h$  is the height along the radius perpendicular to the line of sight,  $R_\odot$  is the radius of the Sun.

The results of numerical calculation using Equation (1) and the intensities shown in Figure 3 are given in Figure 4. It should be noted that this method is used as a rule for the uniform model atmosphere, but it appears to be suitable for

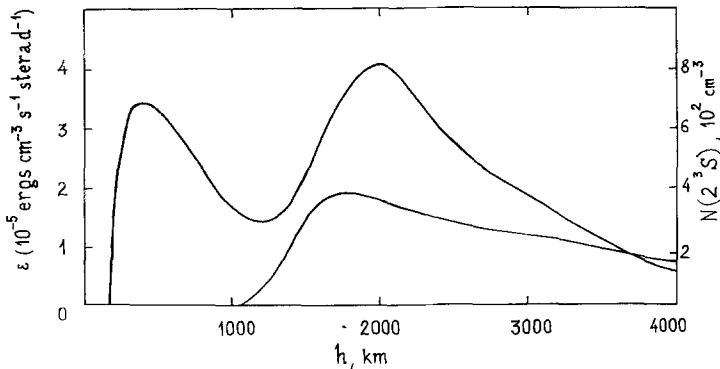


Fig. 4. The emission coefficient  $\epsilon(h)$  and corresponding  $2^3S$  population for the spherically symmetric chromosphere (the lower curve for undisturbed region and the upper one for faint plage).

more general cases as well if the spherical symmetry condition is satisfied. In inhomogeneous models the solution of the Abelian type equation is a number of values averaged over an interval of heights.

It is evident that  $\varepsilon(h)$  is connected with the  $3^3D$  level population by

$$\varepsilon(h) = \frac{1}{4p} N(3^3D) A_{5876} h \nu_{5876}. \quad (2)$$

The noticeable value of the population of a triplet level, particularly of the lowest metastable  $2^3S$  level population, may be caused by electron collision excitation  $1^1S \rightarrow 2^3S$ . Due to a very high excitation potential, this first mechanism requires  $T \geq 25\,000$  K. The second mechanism advanced by a number of authors, particularly Nikolskaya (1966), for spicules, consists in photoionization of He I by coronal XUV radiation with  $\lambda < 504 \text{ \AA}$ . Photoionization is followed by photo-recombination with delay in the metastable state  $2^3S$ . This second mechanism can yield a noticeable population of  $2^3S$  level with sufficient XUV radiation flux even at  $T < 20\,000$  K, when electron collision may be neglected.

Arguments in favour of the second mechanism have been recently advanced by Zirin (1975). Two of these arguments appear to be particularly important. XUV helium lines are weakened in coronal holes and near poles, i.e. in the regions where radiation flux with  $\lambda < 504 \text{ \AA}$  is decreased. There is experimental evidence of maximum  $D_3$  emission. Below the height of this maximum, the decrease of  $D_3$  emission can be connected with a smaller number of photons ionizing He. In addition to Zirin's arguments, it should be noted that from the data of the head of the helium continuum it follows that the temperature is low,  $T \approx 12\,500$  K (Gulyaev, 1972). Moreover, the data for the  $10830 \text{ \AA}$  line on the disk, particularly in plages, are well explained by the second mechanism (Livshits, 1975).

Thus, assuming that the second mechanism is correct, we shall calculate the triplet level populations. When the probability of elementary processes in the triplet system greatly surpasses the rate of departure from triplet levels into the continuum and singlet levels, the relative populations of the triplet levels are determined by two main processes: the photo-excitation by radiation from the photosphere and the spontaneous transitions (Krat *et al.*, 1960). In particular,  $N(2^3S):N(2^3P):N(3^3D) = 0.86:0.14:0.0024$  (see Appendix). Since  $N(3^3D)$  is proportional to  $N(2^3S)$ , the righthand side of axis (see Figure (4) shows  $N(2^3S)$ ).

For the calculation of  $N(2^3S)$  we make use of a simple theory based on the physical concepts of Gulyaev (1968). The ionization fraction equation and the steady state equation for the  $2^3S$  level are as follows (see Appendix):

$$\begin{aligned} N(1^1S) \frac{\varphi(1^1S)}{N_e} &= N(\text{He II})\alpha, \\ N(2^3S) \left[ \frac{\varphi t}{N_e} + q_{ts} \right] &= N(\text{He II})\alpha t, \\ N(1^1S) + N(\text{He II}) &= 0.1N_e. \end{aligned} \quad (3)$$

In (3)  $-\varphi(1^1S)$ ,  $\varphi_t$  are the photoionization rates ( $S^{-1}$ ) for the ground and triplet levels and  $\varphi_r$  allows for the decrease of triplet levels population as one passes from low to high levels.  $\alpha$ ,  $\alpha_t$   $\text{cm}^3 \text{s}^{-1}$  are the rate coefficients for recombination into all He I levels and into triplet levels only.  $q_{ts}$  is the rate coefficient of excitation by electron impact ( $\text{cm}^3 \text{s}^{-1}$ ) from the  $2^3S$  level together into  $2^1P$  and into  $2^1S$  singlet levels. The helium-to-hydrogen abundance ratio is assumed to be 0.1 in number. The second helium ionization was neglected, i.e.  $N(\text{He III}) = 0$ .

From (3) it follows that

$$N(2^3S) = \frac{0.1N_e\alpha_t}{\left[1 + \frac{N_e\alpha}{\varphi(1^1S)}\right] \left[\frac{\varphi_t}{N_e} + q_{ts}\right]}. \quad (4)$$

For the calculation of (4) the recombination rate coefficients at  $T = 20\,000$  K are equal to  $\alpha \approx 2.7 \times 10^{-13} \text{ cm}^3 \text{ s}^{-1}$  and  $\alpha_t \approx 1.2 \times 10^{-13} \text{ cm}^3 \text{ s}^{-1}$  according to Burgess *et al.* (1967). The collision cross sections mentioned by Burke *et al.* (1969) were integrated over a Maxwellian electron distribution for  $T = 20\,000$  K. From there  $q(2^3S - 2^1S) \approx 2.1 \times 10^{-8} \text{ cm}^3 \text{ s}^{-1}$ ,  $q(2^3S - 2^1P) \approx 1.4 \times 10^{-8} \text{ cm}^3 \text{ s}^{-1}$ , and then the total value will be  $q_{ts} \approx 3.5 \times 10^{-8} \text{ cm}^3 \text{ s}^{-1}$ . Photoionization from each level was calculated by means of

$$\varphi = 2\pi \int_{\nu_0}^{\infty} \frac{k}{h\nu} \bar{I}_\nu \, d\nu, \quad (5)$$

where  $k$  is the absorption coefficient, and  $\pi\bar{I}$   $\text{ergs cm}^{-2} \text{ s}^{-1} \text{ Hz}^{-1}$  is the radiation flux near the Sun. The absorption coefficients from the ground state are taken according to Allen (1955); the absorption coefficient from all levels with a principal quantum number of 2 is calculated by Beygman *et al.* (1976). In particular, from  $2^3P$  level  $k = 1.47 \times 10^{-17} (\lambda/\lambda_0)^2$  with  $\lambda_0 = 3430 \text{ \AA} > \lambda > 2000 \text{ \AA}$ .

At  $\lambda < 504 \text{ \AA}$  the radiation flux values are borrowed from Hall and Hinteregger's (1970) absolute measurements. The radiation flux of the photosphere used was that given by Makarova *et al.* (1972). After integration, we get

$$\varphi(1^1S) = 4 \times 10^{-3} \text{ s}^{-3}, \quad \varphi(2^3S) = 500 \text{ s}^{-1}, \quad \varphi(2^3P) = 9.1 \times 10^3 \text{ s}^{-1}.$$

The photoionization rate from all triplet levels (see also Nikolskaya, 1966) proves to be close to

$$\varphi_t = \varphi(2^3S) + \frac{0.14}{0.86} \varphi(2^3P) \approx 1.7 \times 10^3 \text{ s}^{-1}.$$

We calculated the theoretical relation  $N(2^3S)$  to  $N_e$  for three quantities of ionizing radiation flux (Figure 5). Before discussing this question we should mention that we have assumed that the curve 1 with the lowest values of ionizing radiation flux corresponds to an undisturbed region and the curve 2 corresponds to a faint plage. Taking the average value  $N(2^3S) \approx 370 \text{ cm}^{-3}$  for the undisturbed region at  $h = 2000 \text{ km}$  (Figure 4) and curve 1 in Figure 5, we get  $N_e \approx$

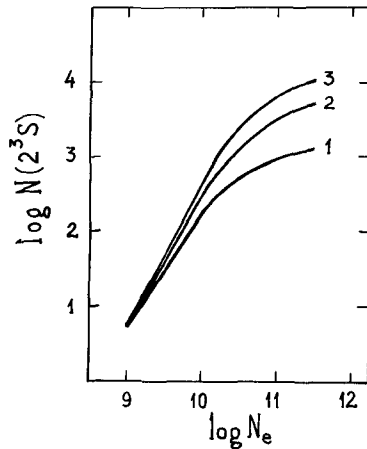


Fig. 5. The density dependence of  $2^3S$  population at  $T=20\,000$  K for three different values of XUV-radiation flux (see the text). The values of XUV-radiation flux in the corona are borrowed from Hall and Hinteregger, 1970 (curve 1), increased by a factor of 3 (curve 2) and by a factor of 10 (curve 3).

$2.1 \times 10^{10} \text{ cm}^{-3}$ . Taking the average value  $N(2^3S) \approx 800 \text{ cm}^{-3}$  for the faint plage at  $h=2000$  km (Figure 4) and from curve 2 in Figure 5, we get the same value  $N_e \approx 2.2 \times 10^{10} \text{ cm}^{-3}$ . As regards  $N_e$  values, we want to emphasize that they are averaged over an interval in the height. It should be noted that the theoretical value of the  $2^3S$  level population depends on  $T$  very little. So, its maximum value decreases less than twice with  $T$  changing from 20 000 K to 10 000 K.

Now we return to the XUV flux ionizing He. It must be estimated at the heights where the helium lines are radiated. Under the assumption of a uniform chromosphere, the flux of XUV radiation will be significantly absorbed by H and He atoms, the number of which in the middle chromosphere is rather large, as shown by the observations. Therefore, the helium emission mechanism under consideration may be applied only to the middle chromosphere consisting of separate features (small filaments, spicules etc). In such a case the XUV radiation in a rarefied space may obviously penetrate between the features down to lower heights. We make rough estimates of the absorption of radiation with  $\lambda < 500 \text{ \AA}$  for Pikelner's (1971) model of the middle chromosphere. In this model, besides spicules, the small filaments-fibrils are considered to be responsible for absorption on the disk in the  $H\alpha$  line and for emission at the limb at 1000–4000 km (henceforth, the term 'fibrils' will be used for small filaments in the given height range in active and undisturbed regions). In Pikelner's model, in the presence of  $L\alpha$ -radiation the hydrogen is highly ionized and the electron density in fibrils decreases from  $N_e \approx 10^{11} \text{ cm}^{-3}$  following the hydrostatic law with  $T \approx 15\,000$  K. Now let us suppose the fibrils project on the disk to occupy 0.1–0.2 of the total surface, and in this case a high absorption of XUV radiation flux begins approximately at the height where  $\tau_{500} \approx 1$  for the fibril itself. Thus, in the layer where



the XUV radiation is absorbed effectively, the flux of radiation, arriving from above, with  $\lambda < 500 \text{ \AA}$ , becomes weaker by a factor of about 3. This estimation is similar to Zirin's (1975) result, where a flux in the range of 230–500  $\text{\AA}$  becomes weaker by a factor of  $[E_2(\tau)]^{-1} \approx 4$  at  $\tau_{500} \approx 1$ . It should be noted that the condition  $\tau_{500} \approx 1$  in fibrils and in Pikelner's model infers that the height of 'effective' absorption of  $\lambda < 500 \text{ \AA}$  radiation is likely to be close to that of the above mentioned maximum of the  $D_3$  He line, i.e. 2000 km.

Being confined to the region about the helium luminosity maximum, we calculated relation (2) using XUV radiation fluxes borrowed from Hall *et al.* (1970) and reduced by a factor of 3. The result is shown by curve 1 in Figure 5 and refers to the undisturbed regions. Taking into account that in plages the fluxes of radiation with  $\lambda < 500 \text{ \AA}$  may be about 10 times as large, the calculations using Equation (2) were also made for the fluxes increased by a factor of 3 and 10 with respect to those adopted for curve 1. The corresponding values of photoionization rate are  $\varphi(1^1S) = 1.3; 4.0; 12 \times 10^{-3} \text{ s}^{-1}$  for curves 1, 2 and 3 respectively. Curves 2 and 3 may be assumed to describe this dependence for faint plage and for plage.

### 3. Discussion

The matter in the middle chromosphere is highly ionized, so that the total number of particles  $N \approx N_p = N_e$ . At  $h = 1000 \text{ km}$ , the electron density  $N_e$  can be reliably determined from the Balmer lines originating on the upper levels and according to Henze (1969) is  $(1-2) \times 10^{11} \text{ cm}^{-3}$ . However, in the middle chromosphere such a determination becomes impossible. Our experimental data for the height range above 1000 km confirm the assumption that the triplet helium emission occurs because of the penetration of XUV-radiation as low as these heights. If it is true, the electron density in the middle chromosphere can be determined from the observations of the  $D_3$  helium line. The solution of the Abelian equations gives  $N_e \approx 2.2 \times 10^{10} \text{ cm}^{-3}$  at  $h = 2000 \text{ km}$ . This figure is, obviously, the average  $N_e$  value along the line of sight; the electron density in fibrils themselves is about twice as large. To construct a detailed model of the middle chromosphere using triplet helium line observations one needs to solve the transfer equation for XUV-radiation and to examine the structural features in a more detailed way.

Following Pikelner's model, we identify the small filaments rising above the limb up to 4000 km with the fibrils and dark fine mottles of the  $H\alpha$ -chromosphere. Then these filaments, when exposed to XUV-radiation, will emit the triplet helium lines. These question of singlet helium lines and radio emission within such a model must be treated separately.

### Appendix

The populations of the bound levels for neutral helium were calculated first of all

in an optically thin model. The excitation and ionization by electron impact, except collisional excitation (or de-excitation)  $2^3S \rightarrow 2^1S$ ,  $2^1P$ ,  $2^3P \rightarrow 2^1S$ ,  $2^1P$ , are not included in this calculation. The steady state equations for triplet He levels will be written as:

$$\begin{aligned}
 N_1\varphi_1 + N_1\Phi_{12} + N_1\Phi_{14} + N_1N_e q_{11'} + N_1N_e q_{12'} \\
 &= N(\text{He II}) N_e\alpha_1 + N_2A_{21} + N_4A_{41}, \\
 N_2A_{21} + N_2\varphi_2 + N_2\Phi_{23} + N_2\Phi_{25} + N_2N_e q_{21'} + N_2N_e q_{22'} \\
 &= N(\text{He II})N_e\alpha_2 + N_1\Phi_{12} + N_3A_{32} + N_5A_{52}, \\
 N_3A_{32} + N_3\varphi_3 &= N(\text{He II})N_e\alpha_3 + N_2\Phi_{23}, \\
 N_4A_{41} + N_4\varphi_4 &= N(\text{He II})N_e\alpha_4 + N_1\Phi_{14}, \\
 N_5A_{52} + N_5\varphi_5 &= N(\text{He II})N_e\alpha_5 + N_2\Phi_{25}.
 \end{aligned} \tag{6}$$

The number of equations in this system is infinite. Level numbers  $m$  and ionization potential at each of the bound levels are listed in Table II. Here we give photo-ionization rates  $\varphi_m$  estimated from Equation (5). Taking cross sections calculated by Burke *et al.* (1969) in the 'close coupling' approximation, we get for  $T = 20\,000\text{ K}$  the following values of excitation rate coefficients by electron impact (in units  $\text{cm}^{-3}\text{ s}^{-1}$ ):

$$\begin{aligned}
 q_{11'} &= 2.1 \times 10^{-8}, & q_{22'} &= 10^{-9}, \\
 q_{12'} &= 1.4 \times 10^{-8}, & q_{1'2} &= 4 \times 10^{-8};
 \end{aligned}$$

and de-excitation rates are respectively:

$$\begin{aligned}
 q_{1'1} &= 10^{-7}, & q_{22'} &= 3.5 \times 10^{-9}, \\
 q_{2'1} &= 3.1 \times 10^{-8}, & q_{21'} &= 0.5 \times 10^{-8}.
 \end{aligned}$$

The calculations of these coefficients made by Beygman *et al.* (1976), using a more general method of orthogonalized wave functions of the external electron, gave values coinciding with the previous ones with an accuracy up to a factor of  $\approx 2$ .

TABLE II  
Ionization potentials and photoionization rates  
for some levels of He I

$m$	Level	$x_m, \text{eV}$	$\varphi_m, \text{s}^{-1}$
0	$1^1S$	24.58	$4.10^{-3}$
1	$2^3S$	4.76	$5.10^2$
2	$2^3P$	3.62	$9.1 \times 10^3$
3	$3^3S$	1.65	$5.6 \times 10^4$
4	$3^3P$	1.65	$5.6 \times 10^4$
5	$3^3D$	1.65	$5.6 \times 10^4$
1'	$2^1S$	3.97	$10^3$
2'	$2^1P$	3.36	$10^4$

They independently confirm the calculations of Burke *et al.* The rates of photo-excitation by radiation from the photosphere can be calculated from:

$$\Phi_{mn} = \frac{g_n}{g_m} A_{nm} \left[ \exp \left( \frac{\Delta\chi}{kT_{\odot}} \right) - 1 \right]^{-1} \times W,$$

where the excitation potential  $\Delta\chi = \chi_m - \chi_n$  can be determined from the table, and the dilution factor  $W \approx \frac{1}{2}$  and the black-body temperature used are as given by Makarova *et al.* (1972).

Since the probability of spontaneous transition from  $2^1P$  to the ground level is large – transition from triplet levels to the ground level being out of the question – the population of singlet levels proved to be much smaller than the population of corresponding triplet levels. For this reason collisional excitation and de-excitation from  $1'$  and  $2'$  to 1 and 2 appear to be negligible.

A specific property of the set of Equations (6) is as follows. Each equation contains terms with  $A$ ,  $\Phi$ , exceeding terms with  $N_e\varphi$ ,  $N_eq$ ,  $N_e\alpha$  by several orders of magnitude. Keeping in every equation only these terms with  $A$ ,  $\Phi$ , we can write:

$$\begin{aligned} N_1\Phi_{12} + N_1\Phi_{14} &= N_2A_{21} + N_4A_{41}, \\ N_2A_{21} + N_2\Phi_{23} + N_2\Phi_{25} &= N_1\Phi_{12} + N_3A_{32} + N_5A_{52}, \\ N_3A_{32} &= N_2\Phi_{23}, \\ N_4A_{41} &= N_1\Phi_{14}, \\ N_5A_{52} &= N_2\Phi_{25}. \end{aligned} \tag{7}$$

It is easily seen that only four of the five equations of the set (7) are linearly independent. In this case we can express the population of any triplet level as a function of the population of any single level, for example  $2^3S$ , or as a function of the sum of all triplet levels population. In particular, from the set (7) we have  $N(2^3S) : N(2^3P) : N(3^3D) = 0.86 : 0.14 : 0.0024$ .

The physical sense of set (7) is evidently as follows. The relative population of triplet levels is due to photo-excitation by radiation from the photosphere and to spontaneous transitions only.

The relation between the population of any triplet level and  $N(\text{He II})$  may be obtained by summarizing all the equations of primary set (6). All the largest terms disappear and we can write:

$$\sum_{m=1}^{\infty} N_m\varphi_m + \sum_{m=1}^2 N_mN_e(q_{m1'} + q_{m2'}) = N(\text{He II})N_e \sum_{m=1}^{\infty} \alpha_m. \tag{8}$$

If we designate

$$\begin{aligned} \alpha_t &= \sum_{m=1}^{\infty} \alpha_m, \\ \varphi_t &= \sum_{m=1}^{\infty} \frac{N_m}{N_1} \varphi_m \approx \varphi_1 + \frac{N_2}{N_1} \varphi_2, \\ q_{ts} &= \sum_{m=1}^2 \frac{N_m}{N_1} (q_{m1'} + q_{m2'}) \approx q_{11'} + q_{12'}, \end{aligned}$$

(approximated equations take into account the above coefficient values), and if we divide (8) by  $N_e$ , we shall get the second equation of the set (3) above.

The ionization fraction equation

$$N_0\varphi_0 + \sum_{m=1'}^{\infty} N_m\varphi_m + \sum_{m=1}^{\infty} N_m\varphi_m = N(\text{He II})N_e(\alpha_0 + \alpha_s + \alpha_t), \quad (9)$$

where the sums from the left-hand side are taken over all singlet and triplet levels respectively and where recombination rate coefficient for all singlet states is

$$\alpha_s = \sum_{m=1'}^{\infty} \alpha_m.$$

Without examining the equation of transfer in the line at 584 Å, we can consider two extreme cases. When the optical thickness at the center of the line at 584 Å becomes very large, the resonance photon is multiply scattered and the effective probability of spontaneous transition sharply falls ( $A_{2'0}\beta < \varphi_{2'}$ , where  $\beta$  is the pure radiative bracket). Then for singlet and triplet states we can write:

$$\begin{aligned} \sum_{m=1'}^{\infty} N_m\varphi_m &= N(\text{He II})N_e\alpha_s, \\ \sum_{m=1}^{\infty} N_m\varphi_m &= N(\text{He II})N_e\alpha_t. \end{aligned} \quad (10)$$

We assume here that excitations and de-excitations between neighbouring singlet and triplet levels are balanced. Substituting (10) in (9) we get:

$$N_0\varphi_0 = N(\text{He II})N_e\alpha_0. \quad (12)$$

In the other extreme case, when  $\tau_{584}$  is not very large, and inelastic scattering from triplet and singlet states is essential, the first addend in the left-hand side of Equation (9) significantly exceeds the other terms. This assumption appears to be true when  $\varphi_2/A_\beta \ll 1$  or  $1 \geq \beta \gg 5 \times 10^{-7}$  for resonance line at 584 Å. (It is easily obtained for a model atom of  $2^1P$  and  $1^1S$  levels only). By neglecting two summations in (9) we obtain the first equation of set (3) above.

Since  $\alpha/\alpha_0 \approx 2$ , the difference between two extreme cases is not very great. From experimental evidence of singlet-triplet ratio in the chromosphere it follows that the second case is more real.

In all the above-mentioned cases we neglected the excitation by electron impact of allowed (dipole) and intercombination transitions if  $T = 20\,000$  K. From equations taken from Livshits (1975) it is easy to see that our suggestion is correct if  $N_e q_{01} < \varphi_0$  and  $N_e q_1 < \varphi_t$  (where  $q_1$  is the collisional ionization rate coefficient from  $2^3S$  level). According to Vainshtein *et al.* (1973), when  $T = 20\,000$  K, we have  $q_1 = 7 \times 10^{-9} \text{ cm}^3 \text{ s}^{-1}$  and  $q_{01} = 6.6 \times 10^{-15} \text{ cm}^3 \text{ s}^{-1}$ . If  $\varphi_0 = 4 \times 10^{-3} \text{ s}^{-1}$  and if  $\varphi_t = 1.7 \times 10^3 \text{ s}^{-1}$ , we shall find that inequalities are fulfilled when  $N_e < 6 \cdot 10^{11} \text{ cm}^{-3}$  and  $N_e < 2.5 \times 10^{11} \text{ cm}^{-3}$ .

## References

- Allen, C. W. A.: 1955, *Astrophysical Quantities*, 1st ed., New York.
- Belkina, I. L. and Dyatel, N. P.: 1972, *Astron. Zh.*, **49**, 588; translation *Soviet Astron.*, **16**, 476.
- Beygman, I. L. and Livshits, M. A.: 1976, *Astron. Zh.* (in press).
- Burgess, A. and Seaton, M. J.: 1960, *Monthly Notices Roy. Astron. Soc.*, **121**, 471.
- Burke, P. G., Cooper, J. W., and Ormonde, S.: 1969, *Phys. Rev.*, **183**, 245.
- Gulyaev, R. A.: 1968, *Solnetshnaja aktivnost*, No. 3, 104.
- Gulyaev, R. A.: 1971, *Solar Phys.*, **18**, 410.
- Gulyaev, R. A.: 1972, *Solar Phys.*, **24**, 72.
- Hall, L. A. and Hinterregger, H. E.: 1970, *J. Geophys. Res.*, **75**, 6959.
- Krat, V. A. and Sobolev, V. M.: 1960, *Izv. Main (Pulkovo) Astron. Obs.*, No. 163, 2.
- Livshits, M. A.: 1975, *Astron. Zh.*, **52**, 970.
- Makarova, E. A. and Kharitonov, A. V.: 1972, *The Energy Distribution in the Solar Spectrum*, Moscow.
- Nickolskaya, K. I.: 1966, *Astron. Zh.*, **43**, 936.
- Pikelner, S. B.: 1971, *Solar Phys.*, **20**, 286.
- Poulain, P.: 1974, *Solar Phys.*, **36**, 339.
- Shilova, N. S.: 1973, *Solnechnye Dannye*, No. 2, 92.
- Sobolev, V. V.: 1967, *Course of Theoretical Astrophysics*, Moscow.
- Vainshtein, L. A., Sobelman, I. I., and Yukov, E. A.: 1973, *The Atoms and Ions Excitation Cross-Sections by Electrons*, Moscow.
- White, O.: 1963, *Astrophys. J.*, **138**, 1316.
- Zirin, H.: 1975, *Big Bear Solar Obs. Preprint No. 0147*.